ACS OMEGA

Open Access

http://pubs.acs.org/journal/acsodf

Article

Isolation of Carbon Black from Soils by Dispersion for Analysis: Quantitation and Characterization by Field Flow Fractionation Techniques

Lorenzo Sanjuan-Navarro, Aaron Boughbina-Portolés, Yolanda Moliner-Martínez, Frank von der Kammer, and Pilar Campíns-Falcó*

Cite This: *ACS Omega* 2023, 8, 34795−34804

Read Online

ACCESS | Metrics & More | Article Recommendations | Supporting Information

ABSTRACT: In the present work, a procedure based on a dispersive medium for carbon black (CB) isolation from soil samples for analysis was proposed for the first time. Polymeric and biological dispersants and a sequential use of both dispersants were assayed. Asymmetrical flow field flow fractionation with dynamic light scattering detector (AF4-DLS) and sedimentation field flow fractionation with multi-angle light scattering detector (SdF3-MALS) were used for CB quantitation and characterization in the achieved dispersions. Soil samples contaminated with CB were processed, and CB isolation depended on the solid size distribution and composition and dispersant nature. More quantitative isolations were achieved for the four soils treated by the biological dispersant. As the organic matter percentage is higher in soil, the CB isolation was better, varying between 75 and 99% with standard deviation (s) $\leqslant$ 2% for all soils. A soil contaminated with a CB-based pigment paste was analyzed, achieving (99 ± 2)% expressed as expanded uncertainty (K = 2) of dispersive isolation by the biological dispersant, and the sampling was scaled to 250 g of soil with positive results. The procedure was completed by CB recovery to obtain a solid residue able to be reused if necessary. For the filter-aided recovery step, different membranes (fiberglass, nylon, and Teflon) with a pore size between 0.1 and 5 μm were tested. The quantitation of the CB retained in the filter was measured by diffuse reflectance spectroscopy. Teflon (0.10 μm) provided better results for CB recovery, and its re-dispersion was also studied with suitable results. Determination of CB from the filters by diffuse reflectance spectrometry provided the same results than AF4 for CB dispersions.

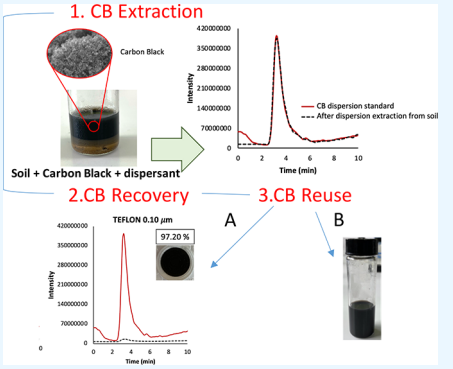

INTRODUCTION

In the recent years, nanomaterials (NMs) have been widely used in different industries and research contexts, making use of their special physical−chemical properties, which mainly depend on their size and composition.[1] NMs inevitably play a key role in environmental and health issues during their life cycle, from synthesis to disposal, due to their increasing global production and application.[2] Thus, methods for their extraction, determination, characterization, and/or elimination or even re-use are required.[3]

Among the different NMs released into the environment, engineered nanoparticles (ENPs) have recently emerged and quickly showed a very fast development.[4] In this field, metallic nanoparticles such as AgNPs or AuNPs[5] and specifically carbon-based nanomaterials (carbon nanotubes (CNTs), fullerenes, and carbon black (CB), among others)[6] represent also an important pollutant source, which should be monitored.

Particularly, carbon black (CB) is an important carbon-based nanomaterial from the industrial point of view with more than 8.1 million metric tonnes produced worldwide.[7] Thus, to monitor CB in the environment and study its behavior and adverse effects, methods to extract CB from soils, sediments, and biota are required as well as methods to further characterize CB from such complex samples.[7−9]

This material consists of a black powder in the form of near spherical particles of colloidal size. It is produced by the incomplete combustion of hydrocarbons under reduced presence of oxygen.[10,11] Surface chemistry, particle size, structure, porosity, or thermal and electronic properties are the principal parameters that allow characterization and classification of this NM. As it is expected, these properties are key parameters for its use and applicability[12,13] but also its toxicity. It has wide applicability and has found uses in fields such as rubbers, tires, inks, paints, printer toners, and electrodes.

Received: June 1, 2023
Accepted: August 8, 2023
Published: September 12, 2023

The presence of CB in aquatic and terrestrial environments could potentially lead to unexpected harmful effects since its behavior in these ecosystems is largely unknown.[14,15] As an example, CB aggregates reduce fertilization success of marine seaweed.[16] Moreover, impact studies of CB materials in marine microcrustacean revealed their toxicity in filter-feeding organisms.[17,18] On the other hand, in the terrestrial environments, CB produces an increase risk to the pristine nature of agricultural ecosystems, threatening terrestrial organism habitats and faunal biodiversity.[2] Earthworm, whose biochemical responses are regarded as an early warning of soil heavy metal and pesticide pollution, may be considerably affected by the presence of this nanomaterial.[19,20] In the same way, potential transition of CB from soil to the atmosphere could induce harmful effects on human health such as cytotoxicity to cells and possible carcinogenic tumors.[21,22] For these reasons, it is necessary to develop reliable extraction and characterization procedures to analyze, remove, recover, and reuse CB from the environment.

CB analysis has been traditionally performed by spectroscopy techniques such as dynamic light scattering (DLS), which allows to establish particle size,[23] and analytical imaging techniques (TEM or SEM) showing a visual identification of material focused on its surface morphology.[24] Nevertheless, separation techniques provide complete information about size distribution and composition of particle dispersions. In this context, asymmetrical flow field flow fractionation (AF4) and sedimentation field flow fractionation (SdF3), have been demonstrated to be a powerful separation strategy in the detection, quantification, and characterization of nanomaterials[9,25,26] from their dispersions. The CB determination in environmental samples is still very scarce and, in the case of some matrices such as soils, is unexplored.[26]

Thus, the objective of the present work was to develop a procedure for CB isolation from soil matrices for analysis. The CB isolation efficiency was evaluated through the study of the Dispersive Isolation Efficiency (D-IE) using biological and polymeric dispersants or even their sequential use. Separation and quantitation of CB in dispersions were performed by asymmetrical flow field flow fractionation coupled to DLS (AF4-DLS) and sedimentation field flow fractionation coupled to MALS (SdF3-MALS). Four soils with differences in particle size distribution and % organic matter were tested, and as a practical application, a soil sample contaminated with a CB-based pigment paste was also analyzed. The sampling was scaled to 250 g of soil to approximate to a real situation in soil analysis. Moreover, Filter-Aided Recovery Efficiency (FA-RE) employing different membranes (fiberglass, nylon, and Teflon) with a variation of pore sizes (0.1 to 5 μm) was also studied to evaluate CB recovery from the obtained dispersions for achieving a solid residue. The CB retained in filters was determined by diffuse reflectance spectroscopy.

RESULTS AND DISCUSSION

CB Isolation from Soils and Quantitation. CB N326 as a target CB-NM and polymeric and biological dispersive agents were employed. Characterization of these dispersions was carried out in a previous study,[27] and results indicated that size distribution was a function of the dispersive media. Average hydrodynamic diameter (d_{hydro}) was lower using biological media than that achieved with polymeric media, obtained by DLS d_{hydro} expressed as mean ± standard deviation (s) of 175 ± 4 and 404 ± 4 nm with polydispersity indexes of 0.242 and 0.192, respectively, representing relatively monodisperse size distributions. Zeta potentials were also different, 23 ± 2 and −19 ± 1 mV for polymeric and biological dispersants, respectively.

In a first step, soil samples were treated with the polymeric and biological dispersants to evaluate the matrix response in the absence of CB. Figure 1a,b shows the AF4-DLS-fractograms obtained for mountain A soil using polymeric and biological dispersants, respectively. As can be seen, for both dispersants, the responses were negligible. Moreover, the scattering signal obtained throughout the whole fractionation was too low to obtain a DLS-based hydrodynamic size. AF4-DLS-fractograms obtained for extraction of orchard A soil using polymeric and biological dispersants (Figure 1c,d, respectively) exhibited a similar profile compared with the mountain A soil. Mountain B and orchard B soils were also studied, and fractograms did not provide a remarkable signal. These results indicated that the different matrices did not interfere in CB fractograms.

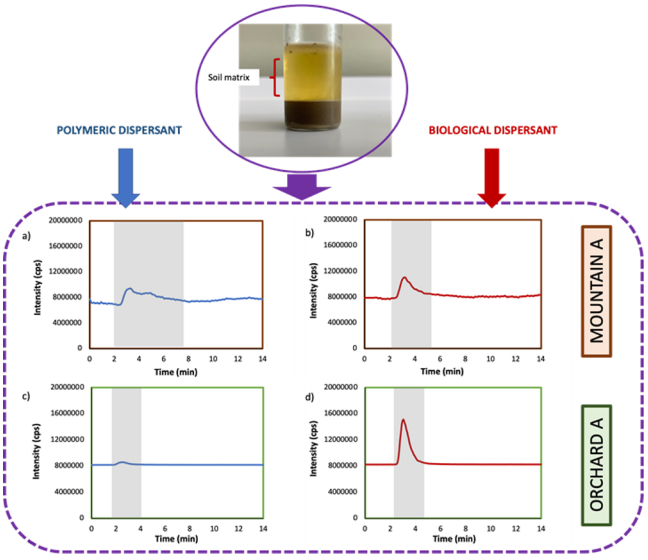

Figure 1. DLS fractograms and d_{hydro} obtained for soil samples. (a) Mountain A soil extracted with a polymeric dispersant. (b) Mountain A soil extracted with biological dispersant. (c) Orchard A soil extracted with a polymeric dispersant. (d) Orchard A soil extracted with a biological dispersant.

Bearing in mind that the LODs achieved by AF4 for CB dispersions prepared from polymeric and biological dispersants are 1.38 and 0.16 mg L^{-1} using area as analytical signals of fractograms,[27] the two mountain (A and B) and two orchard (A and B) soils were spiked with CB and treated employing the procedures described in Materials and Methods.

Figure 2a shows the DLS fractograms obtained for CB isolated from mountain A soil using the polymeric dispersive medium. The D-IE value was 70% as can be seen in Table 1. On the other hand, using the biological dispersive media (Figure 2b), D-IE was 99%, which indicated near-complete isolation of target analyte. The standard deviation (s) values obtained for D-IE were ⩽2% for all experiments as can be seen in Table 1. Orchard A soil showed lower average soil grain size than that corresponding to mountain A soil, 230 and 310 μm, respectively, with a higher particle composition percentage in the range < 100 μm, 17.8 and 3.9%, respectively (see Table S.1 of the Supporting Information).

https://doi.org/10.1021/acsomega.3c03857
ACS Omega 2023, 8, 34795−34804

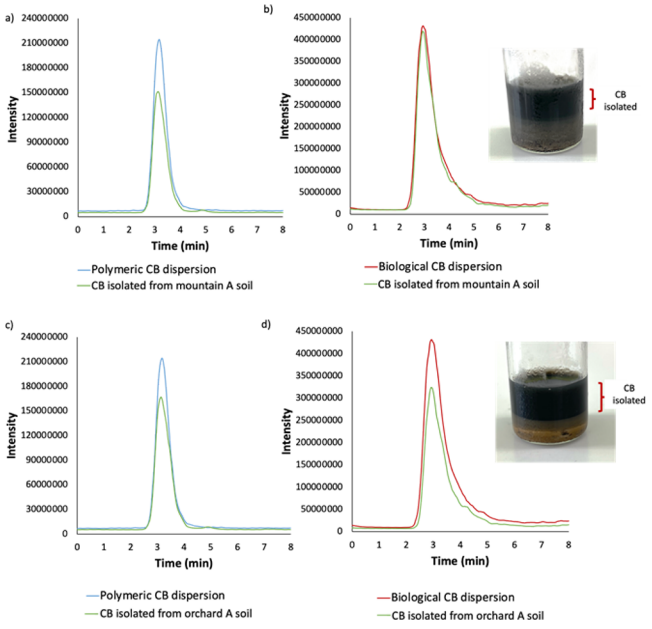

Figure 2. (a) Fractogram for CB isolation from mountain A soil using a polymeric dispersant (compared with CB bulk dispersion in the studied dispersant). (b) Fractogram for CB isolation from mountain A soil using a biological dispersant (compared with CB bulk dispersion in the studied dispersant). (c) Fractogram for CB isolation from orchard A soil using a polymeric dispersant (compared with CB bulk dispersion in the studied dispersant). (d) Fractogram for CB isolation from orchard A soil using a biological dispersant (compared with CB bulk dispersion in the studied dispersant).

Table 1. D-IE: Isolation Efficiencies after the Dispersive Procedure[a]

		soil-dispersed CB	
soil	dispersant	%D-IE ± s	size ± s (nm)
mountain A	polymeric	70 ± 2	399 ± 7; 404 ± 5*
	biological	98.7 ± 1.1	177 ± 3; 168 ± 2*
	sequential polymeric–biological	97.9 ± 1.9	182 ± 2
orchard A	polymeric	73 ± 2	380 ± 6; 391 ± 4*
	biological	75.1 ± 1.8	208 ± 3; 204 ± 5*
	sequential polymeric–biological	64 ± 2	213 ± 7
mountain B	polymeric	62.9 ± 1.4	409 ± 4
	biological	99.1 ± 0.8	169 ± 5
orchard B	polymeric	66 ± 3	385 ± 3
	biological	96.2 ± 1.3	171 ± 4

[a]Hydrodynamic sizes obtained for CB dispersed from fractograms obtained by AF4-DLS. *, batch DLS. Standard deviation = s.

In the case of CB isolated from mountain soil A, for the polymeric dispersant, the average size was 399 nm (see Table 2) and zeta-potential obtained from DLS of 19.5 ± 1.3 mV. In the case of the biological dispersant, the values were 177 nm and −17.1 ± 1.2 mV, respectively. These results indicated that the isolation mechanism for CB present in mountain A soil provided similar results than CB standard dispersions, which means that the soil matrix did not induce a matrix effect on CB properties and stability.

Table 2. Filter-Aided Recovery Efficiency (FA-RE) Values Obtained with the Filter Membranes and in Both Dispersive Media[a]

	dispersive medium FA-RE %: mean value ± s	
membrane	polymeric	biological
fiberglass (2.00 μm)	96 ± 2	2.6 ± 0.1
fiberglass (1.00 μm)	96 ± 2	1.1 ± 0.3
fiberglass (0.70 μm)		4.80 ± 0.14
nylon (5.00 μm)	29.9 ± 0.6	
nylon (0.45 μm)	96 ± 2	11.1 ± 0.7
nylon (0.22 μm)		84.9 ± 1.1
Teflon (0.45 μm)	97 ± 2	5.6 ± 0.4
Teflon (0.20 μm)		65.2 ± 1.4
Teflon (0.10 μm)	99.1 ± 0.7	97.2 ± 2

[a]Standard deviation = s.

Figure 2c ,d shows the DLS fractograms obtained for CB isolation from orchard A soil using polymeric and biological dispersive media, respectively. As can be seen, in this case, the extraction was 75% by using the latter dispersant. Zeta potentials obtained from DLS were 3.2 ± 1.1 mV for polymeric dispersion and −2.4 ± 0.8 mV for biological dispersion, and changes in size were also observed in reference to standard dispersions (Table 1). This fact is in accordance with possible co-extraction of matrix components from soil, which modified the CB capping surface. With a lower amount of organic matter in the soil composition (see Table S.2), the lower CB recovery in the dispersion is achieved (95−99% vs 75%), which can be related to the presence of a higher amount of humic acids in mountain A in reference to orchard A, which enhanced the stability of the dispersion.[28] In addition, it is described that soil organic matter (SOM) was found to create unfavorable conditions for the retention.[29]

The same study was performed for mountain B and orchard B soils, and isolation efficiencies after the dispersion procedure were similar than those obtained for mountain A soil (see Table 1). In these three soil samples, the presence of lower percentage of soil grains <100 μm and higher amount of organic matter near 20% (see Tables S.1 and S.2) allowed to improve the D-IE using a biological dispersant.

A sequential capping exchange study was also carried out; CB was isolated from mountain A soil using a polymeric dispersant (Figure S.2a shows the AF4-DLS signal obtained). Subsequently, CB settling was achieved after centrifugation and sedimentation. The polymeric dispersant was removed, and CB was redispersed with the biological dispersant (see Materials and Methods). As can be seen, the separation profiles were similar to those observed with the biological dispersion; particle size and zeta potential were in concordance with initial values too. For orchard soil A (see Figure S.2b), similar results were obtained with both dispersants, showing lower differences between initial isolation and re-isolation procedure. Thus, it was demonstrated that capping exchange can be performed and that the soil matrix did not interfere in that capping-exchanged isolation step; only a minor increase in the particle size was observed as it is reported in Table 1.

The retention of CB on the surface of the different membranes was measured by AF4-DLS. Figures S.3 and S.4 show the fractograms obtained after the filtration step with both dispersive media. Table 2 summarizes the FA-RE after the filter-aided step obtained for each membrane; the amount of

https://doi.org/10.1021/acsomega.3c03857
ACS Omega 2023, 8, 34795−34804

CB retained depended on CB d_{hydro}, membrane nature, and pore size and type of dispersant. Standard deviation values obtained for FA-RE were ⩽2% for all experiments as can be seen in Table 2.

The use of the polymeric dispersive media resulted in quantitative recovery values, except for the highest membrane pore size of 5 μm. High electrostatic interaction between the fiberglass support and the polymeric dispersant took place considering the different surface charge present to each of them, negative for filter[30,31] and positive for dispersion. In the case of nylon (0.45 μm) and Teflon filters, the average particle size of dispersions (Table 1) was similar or higher than the pore size of filter, generating a complete recovery.

As can be seen in Table 2 and Figure S.4, the behavior of the biological dispersion differed from that provided by the polymeric dispersions. By using fiberglass filters with a pore size larger than or equal to 0.70 μm, CB particles were poorly recovered because the d_{hydro} of these particles was lower than 176 nm and electrostatic interactions between particles and filter support were rather repulsive. The charge surface of both CB and fiberglass material was negative. DLS measurements of filtered solution using fiberglass (2.00, 1.00, and 0.70 μm) and nylon (0.45 μm) suggested an average value of 165 ± 6 nm, which is in concordance with the d_{hydro} observed before the filter-based step.

For nylon filter (0.45 μm), the retention was negligible; however, by using nylon (0.22 μm), retention of CB increased due to the recovery of larger particles and the presence of electrostatic interactions that may occur between nylon material and CB dispersion with opposite charge.[32] In the case of nylon (0.22 μm), the average size obtained for the collected dispersion was 119 ± 4 nm. Therefore, it can be assessed that filtration did not produce significant variations in the hydrodynamic particle size of the dispersion for filters with a pore size greater than or equal to 0.45 μm. For Teflon filter, the results were in concordance with the other materials. Employing Teflon (0.45 μm), a poor efficiency was observed, but if the pore size was reduced down to 0.2 μm, the efficiency increased, taking into account the d_{hydro} of CB. For this last membrane pore size, the average CB size was 115 ± 2 nm. For all assays carried out without quantitative filter recovery, zeta potential analysis was measured, obtaining similar values to the initial bulk dispersion (−16.2 ± 0.7 mV). Using 0.1 μm Teflon filter, the retention was quantitative, since the d_{hydro} was higher than the pore size of filter.

The proposed filter-aided recovery method was evaluated using the isolated CB dispersions obtained from soil samples. Figure 3 shows the fractograms obtained after the recovery step for mountain A and orchard A soils using the studied dispersants. Subsequently, for mountain A soil, using a polymeric dispersant (Figure 3a), CB was recovered by the filter-aided step using fiberglass (2 μm) and Teflon (0.10 μm) as supports. In both cases, no responses in DLS were observed at the retention times, which indicated a quantitative retention of the CB on the surface of the filter membrane. However, for the biological dispersant in the same soil matrix, the CB FA-RE provided quantitative values only with Teflon (0.10 μm) as Table 3 shows and as previously stablished for CB standard dispersions.

Indeed, for orchard A soil, the same study was carried out. Using fiberglass (2 μm) as a support, the FA-RE was 52% (see Table 3) due to the presence of matrix components that induced CB capping modification, changing the retention

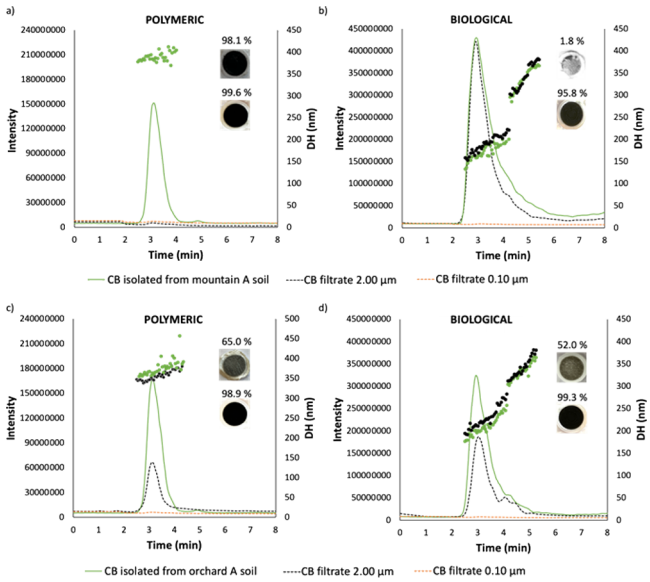

Figure 3. In green: fractograms for CB isolation from different soils using the studied dispersants. Dotted lines: AF4-DLS signal of filtrate using fiberglass (2 μm) (black) and Teflon (0.10 μm) (orange). (a) Study using mountain A soil and polymeric dispersant. (b) Study using mountain A soil and biological dispersant. (c) Study using orchard A soil and polymeric dispersant. (d) Study using orchard A soil and biological dispersant. The insets corresponded to recovered CB from dispersions by fiberglass (2.00 μm) and Teflon (0.10 μm) filters for all dispersions.

Table 3. FA-RE: Efficiencies after the Isolation and Subsequent Filter-Aided Recovery[a]

		CB fiberglass (2.00 μm)		CB Teflon (0.10 μm)
soil	media	% FA-RE ± s	size ± s (nm)	% FA-RE ± s, % redispersion
mountain A	polymeric	98 ± 2		99.6 ± 0.4, 57 ± 2
	biological	1.8 ± 0.2	186 ± 3	95.8 ± 0.8, 77 ± 5
	sequential polymeric–biological	9.7 ± 0.6	180 ± 3	
orchard A	polymeric	65 ± 3	367 ± 6	98.9 ± 1.1, 52 ± 2
	biological	52 ± 1.8	218 ± 5	99.3 ± 0.5, 70 ± 3
	sequential polymeric–biological	48.1 ± 1.1	222 ± 4	

[a]Hydrodynamic sizes obtained for CB dispersion residue after filter-aided recovery. Fiberglass (2 μm) and Teflon (0.10 μm) were studied using polymeric and biological dispersive agents. Standard deviation = s.

behavior (Figure 3c,d). The polymeric dispersion showed similar results. It should be noted that FA-RE was indirectly estimated by measuring CB in the filtered solution by AF4-DLS. The standard deviation values obtained for FA-RE were ⩽5 for all experiments as can be seen in Table 3.

As expected, Teflon (0.10 μm) provided quantitative FA-RE. Table 4 shows FA-RE values for CB dispersions obtained from soils. Percentages of redispersion capacity obtained from solid CB retained in filters are also depicted. These results indicated that the CB extracted can be re-used in two forms: retained in

https://doi.org/10.1021/acsomega.3c03857
ACS Omega 2023, 8, 34795−34804

Table 4. CB Concentration and % Recovery in Different Matrices Calculated on the Surface of the Filter Membrane[a]

CB isolated + filter recovered	concentration ± s ($mg{\cdot}L^{-1}$)	recovery ± s (%)
mountain A soil	37.3 ± 0.6	99 ± 2
orchard A soil	29.6 ± 0.5	79.4 ± 1.6

[a]Standard deviation = s.

the filter or as dispersion. The filter-aided step was also carried out in the sequential capping exchange study, and similar results than those provided by the biological dispersant were obtained (Table 4 and Figure S.2).

SdF3-MALS was also used for measuring dispersions. First, dispersions of the soils shown in Figure 1 for AF4-DLS were measured and a similar conclusion was established: the matrix soil did not give a significant signal. Figure 4 shows the

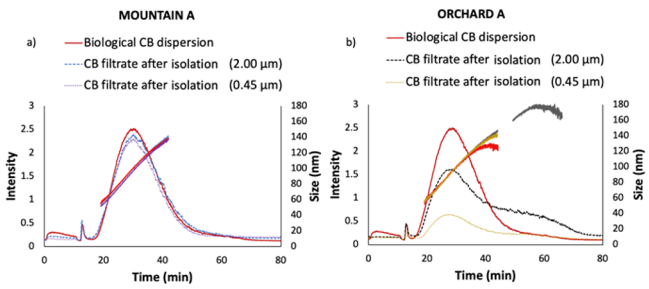

Figure 4. Fractograms for CB dispersion for (a) mountain A soil and (b) orchard A soil using a biological dispersant by SdF3-MALS (red). Dotted lines: SdF3-MALS signals of CB filtrate dispersion after isolation using fiberglass (2 μm) and nylon (0.45 μm) (isolation from mountain soil) and particle geometric radius for the sphere model.

fractograms for CB biological dispersions and the achieved CB dispersions from soils. Figure 4a shows that the recovery of CB from mountain A soil is quantitative, and the particle geometric ratio was 97 ± 3 nm. These results are similar to those shown in Figure 3b obtained by AF4-DLS. Figure 4b gives the fractograms for orchard A soil dispersions after filtration with 2.00 and 0.45 μm filters, and the recoveries were not quantitative as in Figure 3d obtained by AF4-DLS. In both cases, geometric radii were constant for the particle distribution at t_r = 28.7 min: 98 ± 5 and 96.3 ± 1.4 nm for 2.00 and 0.45 μm filters, respectively. The first filter provided a wide distribution around t_r = 46−60 min too with a radius of 174.1 ± 0.9 nm. Those results are similar to those given in Figure 3.

To quantify the CB obtained by the filter-aided recovery method in Teflon membranes (0.10 μm), diffuse reflectance (DR) spectrometry was used by measuring the membrane. DR, measured as absorbance, can be observed in Figure 5. This figure includes the registers of the dispersions of the soils without CB. We used 650 nm for quantitation of the CB isolated because it is selective for CB for both soils.

As can be seen, for mountain A soil, the signal for a CB standard biological dispersion was similar to the signal of CB recovered from soil, which can be related to a quantitative dispersion of the NM (Figure 5a). For orchard A soil, the signal of CB that underwent isolation and filter-aided recovery from soil was slightly lower than the CB recovered from standard dispersion (Figure 5b). Those results are in accordance with those provided by AF4-DLS and SdF3-MALS.

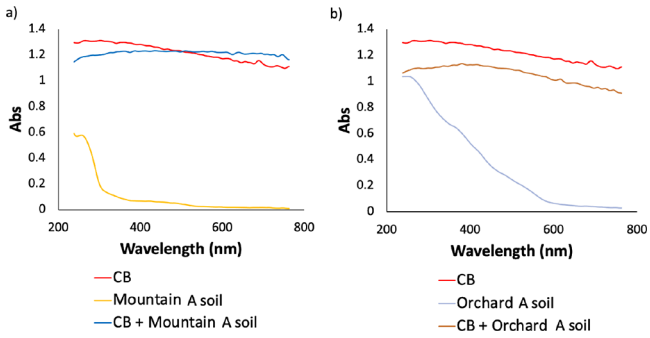

Figure 5. (a) Diffuse reflectance study for CB isolated from mountain soil and recovered using the Teflon membrane (0.10 μm) (CB directly recovered (red), soil extract recovered (yellow), and CB isolated from soil and recovered (blue)). (b) Diffuse reflectance study for CB isolated from orchard soil and recovered using the Teflon membrane (0.10 μm) (CB directly recovered (red), soil extract recovered (gray), and CB isolated from soil and recovered (brown)).

Table 4 shows the concentration values estimated after the CB isolation and filter-aided recovery step using Teflon (0.10 μm). The concentration was established by using the previously calculated calibration curve $A = (0.027 \pm 0.002)[CB] + (0.09 \pm 0.06)$; R^2 = 0.9 and LOD = 0.25 $mg{\cdot}L^{-1}$ (estimated as $3{\cdot}s_{blank}$/slope). The standard deviation values obtained for recoveries were ⩽2% for all experiments as can be seen in Table 4. These results are in accordance with those shown in Table 1.

Pigment Paste Quantification in Soils. As a practical application, an industrial CB-based pigment paste was studied as a potential pollutant of mountain A soil. Figure 6a shows the

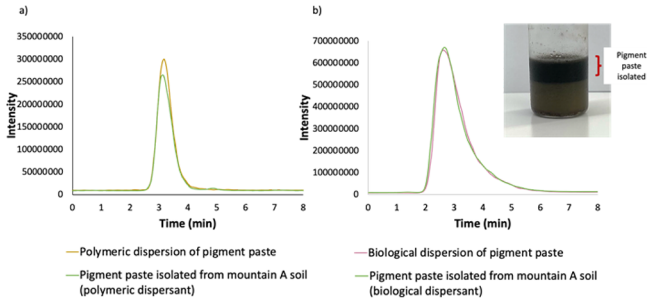

Figure 6. (a) Fractogram for pigment paste isolation from mountain A soil using a polymeric dispersant (compared with a bulk dispersion of pigment paste in the studied dispersant). (b) Fractogram for pigment paste isolation from mountain A soil using a biological dispersant (compared with a bulk dispersion of pigment paste in the studied dispersant).

DLS fractograms of CB isolated from soil and direct pigment paste bulk dispersion using a polymeric dispersant; 88.4% of target analyte was dispersed from soil. Average particle sizes were 312 ± 3 nm for pigment paste isolated from soil and 309 ± 4 nm for direct pigment paste standard dispersion.

In the case of the biological dispersive media, DLS fractograms can be seen in Figure 6b; the isolation (D-IE) was quantitative (99 ± 2)% expressed as expanded uncertainty (K = 2),[33] and average particle sizes were 106 ± 2 nm for direct pigment paste bulk dispersion and 103 ± 4 nm for pigment paste dispersion from soil. The proposed CB isolation procedure was satisfactorily applied to soil contaminated with the pigment paste.

https://doi.org/10.1021/acsomega.3c03857
ACS Omega 2023, 8, 34795−34804

Figure 7a,b shows AF4-DLS fractograms of pigment paste isolated from mountain soil A by using polymeric and

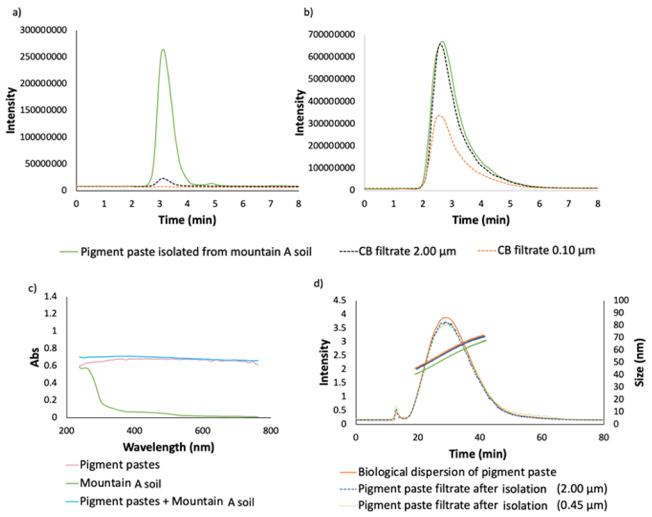

Figure 7. (a) Fractogram for pigment paste isolation from mountain A soil using a polymeric dispersant (green). Dotted lines: AF4-DLS signal of filtrate using fiberglass (2 μm) (black) and Teflon (0.10 μm) (orange). (b) Fractogram for pigment paste isolation from mountain A soil using a biological dispersant (green). Dotted lines: AF4-DLS signal of filtrate using fiberglass (2 μm) (black) and Teflon (0.10 μm) (orange). (c) Diffuse reflectance: absorbance of the samples (pigment paste, mountain A soil, and pigment paste isolated from soil). (d) Fractogram for pigment paste dispersion using a biological dispersant by SdF3-MALS (red). Dotted lines: SdF3-MALS signals of pigment paste filtrate dispersion after isolation using fiberglass (2 μm) (blue) and nylon (0.45 μm) (green) (isolation from mountain soil). Particle geometric radius for the sphere model.

biological dispersants and the resulting dispersions by filtration using fiberglass (2 μm) and Teflon (0.10 μm) filters. As expected in accordance with previous section results, the FA-RE values obtained for the two filters for the polymeric dispersant were near 100% (Figure 7a). For isolated pigment paste dispersion using a biological dispersant (Figure 7b), the retention of target analyte in fiberglass (2 μm) was negligible (very low FA-RE, 2.15%), in accordance with the hydrodynamic size of particles. Meanwhile, using Teflon (0.10 μm) filter, a fraction of CB was retained; however, a residual CB concentration was detected in the filtered solution (48%) due to the presence of a CB distribution with a d_{hydro} = 90 ± 5 nm, which was not retained in the membrane.

DR measurements of the membrane surface (Teflon, 0.10 μm) were also measured to evaluate the concentration and FA-RE in the pigment paste sample as an accuracy confirmation study. Responses of mountain A soil dispersion recovery and direct pigment paste bulk dispersion after the filter-aided step can be seen in Figure 7c. The absorbance spectra showed comparative signals for recovered CB from pigment paste in soil and CB from standard pigment paste dispersion. However, these values were significantly lower than the recovered signal of CB dispersion directly measured at the same concentration level according to the limited retention on the filter support. The concentration value estimated after the pigment paste isolation from mountain A soil and filter-aided recovery step using Teflon (0.10 μm) was 20.4 ± 0.3 mg·L^{-1} with a recovery of 54.5 ± 1.1%, which is in accordance with those provided by dispersion measurements by AF4-DLS, confirming the accuracy of the results.

CB-based pigment paste bulk dispersion and the filtered solution after the recovery step from mountain A soil using a biological dispersant were also analyzed by SdF3-MALS for accuracy validation. Fractograms obtained are shown in Figure 7d. As in the case of CB dispersion for this matrix, isolation was quantitative and the filter-aided recovery step did not produce significant retention on the membrane. The average particle geometric radii obtained were 58.3 ± 1.8 nm for pigment paste bulk dispersion, 59 ± 4 nm for pigment paste isolated and filtered with fiberglass (2.00 μm), and 50.2 ± 0.9 nm for pigment paste isolated and filtered with nylon (0.45 μm). As can be seen, the recovery values and particle radius obtained with SdF3-MALS were in concordance with results observed with AF4-DLS.

For scaling the sampling step, 250 g of an orchard soil was contaminated with 1 mL of the pigment paste as Figure 8

Figure 8. Photographs of the sampling procedure for evaluating the presence of CB in 250 g of solid contaminated with pigment paste. For more details, see the text.

shows. After mixing, the sample is quartered as depicted in Figure 8 and sampled in four portions of approximately 5 g each (S1, S2, S3, and S4 quarters), from which 1 g was taken in duplicate and analyzed as indicated in Materials and Methods for studying the distribution of CB in the sample.

Figure 9 shows the UV−vis fractograms obtained at 450 and 600 nm for the extracts with a biological dispersant of a 1 g sample of the second quarter of Figure 8 and 1 g of orchard soil. As can be seen, the measurements are selective at 600 nm for CB, which is in accordance with the reflectance spectra of the soil, which can be seen in the inset of this figure. The

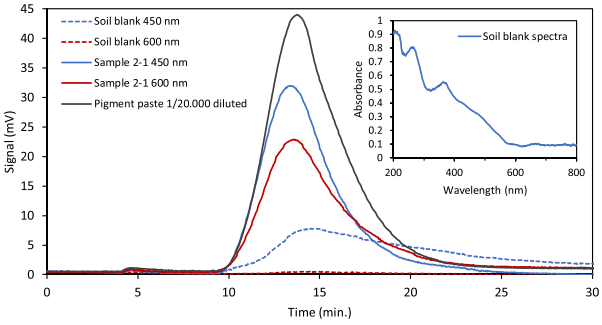

Figure 9. Fractograms obtained for the extracts of orchard soil with and without CB with a biological dispersant at wavelengths of 450 and 600 nm and pigment paste dispersion. The inset gives the reflectance diffuse spectra of the soil.

https://doi.org/10.1021/acsomega.3c03857
ACS Omega 2023, 8, 34795−34804

retention times for the peaks for CB solid dispersions are the same than that obtained with a dispersion of pigment paste.

The distribution of the CB in the soil as can be seen in Figure 10 is not homogeneous; differences in peak area related

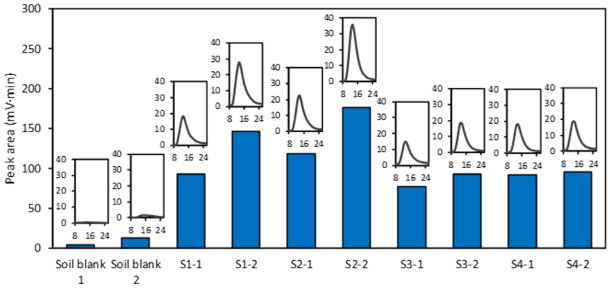

Figure 10. Comparison of the peak areas obtained in the fractograms of different fractions of the sampling given in Figure 8 of the contaminated soil sample and two soil blanks. The insets correspond to the fractograms obtained at 600 nm. S1, S2, S3, and S4 are the four quarters for the two portions analyzed.

to concentration is observed in intra- (for S1 and S2) and inter-quarters. In all portions analyzed, CB was present. The standard deviation obtained for S3- and S4-analyzed quarters was ⩽2%.

CONCLUSIONS

In this work, on-line AF4 coupled to DLS or UV−vis detectors and SdF3 coupled to MALS were employed to study and evaluate a dispersive procedure for extraction and isolation CB from soil samples for analysis. Previously, CB isolation from soils was evaluated. Four different soils (two mountains and two orchard soils) with different characteristics were tested. DLS fractograms indicated quantitative results for mountain A and B and orchard B soils using a biological dispersant and, for orchard A soil, a value of 75%. For the polymeric dispersant, the isolation was near 70%. The different performance between used soils can be related to the lower particle sizes of orchard A soil and the higher concentration of organic matter present in mountain A and B and orchard B soils, which can improve the CB dispersion stability.

A filter-aided process for CB recovery from achieved dispersions was evaluated for quantifying CB from diffuse reflectance spectroscopy and for achieving a solid residue capable of being re-used if necessary. The results indicated that the CB particle size of the dispersion is a key parameter, which depended on the dispersant used. But also, surface charges of the filter must be considered to achieve good recovery. Therefore, the mechanisms governing this filter approach were steric hindrance and electrostatic interactions. Polymeric dispersions resulted in quantitative recoveries for all assayed filters: fiberglass (0.7, 1, and 2 μm), nylon (0.22, 0.45, and 5 μm), and Teflon (0.1, 0.2, and 0.45 μm), except for nylon (5 μm). However, for biological recoveries, up to 10% was achieved using membranes with a pore size >0.45 μm for all materials. These results can be explained considering the hydrodynamic size and z-potential of CB dispersions and nature of the filter besides pore size. For Teflon (0.10 μm) filter, the recovery was complete in all scenarios according to the hydrodynamic size of particles. Results obtained with SdF3-MALS were in concordance with values given by AF4-DLS. Moreover, diffuse reflectance results were used for quantifying the CB recovery in Teflon membranes (0.10 μm), supporting the quantitative isolation from the soil too.

The use of pigment paste as a CB sample provided suitable NM isolation in mountain and orchard soils. In this case, the average hydrodynamic size was near 100 nm, which produced a minor recovery in Teflon (0.10 μm) filter. A sampling strategy for 250 g of soil analyzed by AF4 indicated that the distribution of the pigment paste is not homogeneous in contaminated soils.

MATERIALS AND METHODS

Reagents and Materials. CB (N326) was obtained from Birla Carbon (Cantabria, Spain). Pigment paste was purchased from Pinturas Isaval (Valencia, Spain). Styrene and acrylic acid were used for preparing the polymeric dispersant (Sigma-Aldrich, Missouri, EEUU). Cellular culture medium DMEM/F-12 Modified (supplemented with L-alanyl-L-glutamine dipeptide) provided by Merck (Darmstadt, Germany) was used as the biological dispersant, which also contained Tween 80 (Merck, Darmstadt, Germany).

AF4-DLS liquid carrier was prepared with NaN3 (0.02%) (Panreac, Barcelona, Spain). Melpers 0045 (1%) (BASF, Ludwigshafen am Rhein, Germany) was used as SdF3-MALS carrier solution. Methanol (VWR, Pennsylvania, EEUU) was used for cleaning field flow fractionation systems. For all experiments, water was purified through a Barnstead Nanopure II system.

For FA-EE, membranes of different materials and pore size were used: fiberglass filter of 2, 1, and 0.7 μm (Merck, Darmstadt, Germany), nylon filter of 0.22 and 0.45 μm (Labbox, Barcelona, Spain) and 5 μm (Filterlab, Barcelona, Spain), and Teflon filter of 0.1 μm (Postnova Analytics Inc., Landsberg am Lech, Germany) and 0.20 and 0.45 μm (Merck, Darmstadt, Germany).

Instrumentation. AF4 measurements were performed using an AF2000 MT model purchased from Postnova Analytics Inc. (Landsberg am Lech, Germany). The channel was 29 cm long with a 10 kDa regenerated cellulose membrane and 350 μm channel spacer. The flows were provided by two separate pumps, and the cross-flow was achieved by a separate piston pump, which is constantly adjustable. For all AF4 analyses, the liquid carrier was high-purity Milli-Q water containing 0.02% sodium azide. The injection volume was 20 μL with an injection flow rate of 0.20 mL·min^{-1} and injection time of 3 min. Dispersions were ultrasonicated for 5 min before each injection. The focus flow was 1.30 mL·min^{-1}, and the detection flow remained at 0.5 mL·min^{-1}. Optimal separation conditions were achieved using 0.5 mL·min^{-1} initial cross-flow with a linear decay of 0.0 mL·min^{-1} in 30 min and then held at 0.0 mL·min^{-1} for further 10 min. All samples were analyzed in duplicate (n = 2).

The AF4 system was coupled online with a DLS detector with temperature control (Nano-ZS, Malvern, UK). For DLS detection, the AF4 system was directly interfaced to a Zetasizer without channel split and the detector flow was set to 0.5 mL·min^{-1} for all fractions.

The SdF3 system (CF2000 model, Postnova Analytics Inc., Landsberg, Germany) equipped with a UV/DAD detector (Agilent 1200 series, Agilent Technologies Germany GmbH & Co. KG, Landsberg, Germany), HELEOS II MALS detector, and Astra V was used for data acquisition and treatment (Wyatt Technology, Dernbach, Germany). The SdF3 channel was 57.6 cm long, 2.0 cm wide, and 0.250 mm thick, with a

https://doi.org/10.1021/acsomega.3c03857
ACS Omega 2023, 8, 34795−34804

rotor radius of 15.1 cm. The channel volume was calculated to be 2.7 mL. The carrier solution was introduced into the SdF3 channel by an isocratic pump (model PN1130, Postnova Analytics Inc). The injection volume was 20 μL, and the flow rate was kept constant at 1 mL·min^{-1} for all analyses. The starting rotation speed of the channel was set up at 2250 rpm for relaxation time. This rotation was maintained for the first 5 min of the elution step. After that, the speed decreased to 50 rpm with an exponential field-decay function with an exponent of 0.17. Finally, the rotation was kept for 20 min at 50 rpm. All samples were analyzed in duplicate (n = 2).

Morphology was studied with a Hitachi S-4800 scanning electron microscope at an accelerating voltage of 10.0 keV over a metalized CB solid sample with a mixture of gold and palladium during 30 s.

An optical microscope (ECLIPSE E200 Microscope, Nikon, Amsterdam, Netherlands) was used to obtain the particle soil composition.[5]

Absorbance measurements were carried out using a Cary 60 UV−vis spectrophotometer (Agilent Technologies, California, USA) equipped with a diffuse reflection probe from Harrick Scientific Products (Pleasantville, New York, USA). The diffuse reflection probe has an integral video camera, which provides a visual image to select the sample spot to be analyzed. The spectra were recorded from 200 to 800 nm.

CB Dispersions by Using Polymeric and Biological Media. Polymeric dispersive solvent was a mixture of styrene:acrylic acid (3:1; 0.025%) in water. CB dispersion was prepared after 5 days of dispersant preparation to avoid undesirable responses from the dispersant. A CB dispersion (300 mg·L^{-1}) was prepared. For this aim, the dispersant and the adequate amount of CB were mixed and agitated for 5 min. After, this dispersion was sonicated for 2 h. The working dispersion diluted 1/2 (150 mg·L^{-1}) with the tested dispersant was prepared by adequate dilution and sonicated for 30 min.

The biological dispersive agent was an aqueous solution containing Tween 80 (0.02%) and DMEM/F-12 supplemented (10%). CB dispersions (300 mg·L^{-1}) of each CB sample were prepared following the same procedure described for polymeric dispersions. Dilution 1/8 (37.5 mg·L^{-1}) of these bulk dispersions was prepared using the biological dispersant. The analysis with SdF3-MALS was performed with 100 mg·L^{-1} CB dispersions employing the biological dispersant. Dispersions up to 100 mg·L^{-1} were prepared to obtain a calibration graph and LOD.

Dispersive Isolation from Soil Samples. Two orchard (A and B) and two mountain (A and B) soils were used, and 2 mg of CB was a mixture with 1 g of soil. Then, the dispersions were performed following the procedure mentioned above (5 min agitated + 2 h sonicated). The supernatant was collected and injected in the AF4 system to study the isolation capacity and the potential interferents present in soil samples with the corresponding dilutions (1/2 for polymeric dispersions and 1/8 for biological dispersions).

As a practical application, a soil sample contaminated with a 20% CB-based pigment paste supplied by PINTURAS ISAVAL SL was analyzed. For this aim, 1 mL of the pigment was mixed with 1 mL of the dispersive agents. Then, 25 μL of that dispersion was added to 1 g of soil. Hereafter, CB was isolated and detected following the same steps described above. Another experiment was carried out for scaling the sampling step: 1 mL of the pigment was directly added to 250 g of soil as Figure 8 shows. After mixing, the sample is quartered as depicted in Figure 8, resulting in four representative portions of approximately 5 g each, from which 1 g was taken in duplicate and processed as indicated above. Table 5 gives the used conditions for AF4 analysis.

Table 5. Optimal Instrumental Variables and Conditions of the AF4 System for the Study of CB-NP Dispersions from 250 g of Soil Contaminated with CB

channel parameters	length		long channel (290 nm)		
	spacer		30 μm thick		
membrane	type		regenerated cellulose		
	MWCO		10 kDa		
carrier liquid			NaN_3, 0.02% (w/v)		
flows	injection flow (I_F)		0.20 mL·min^{-1}		
	focus flow		3.30 mL·min^{-1}		
	initial cross-flow (C_F)		3.0 mL·min^{-1}		
times	focus time (F_T)		3.0 min		
injection	type		manual		
	volume		18.8 μL		
detectors			DLS and UV−vis (450 and 600 nm)		
sequence	mode		length, min	C_F, mL·min^{-1}	gradient
		(1) injection + focus	3.0	3.0	
		(2) transition	1.0	3.0	
		(3) elution	4.5	3.0	
		(4) elution	0.25	3.0 to 0.3	linear
		(5) elution	5.0	0.30 to 0.015	exp. (0.5)
		(6) elution	25	0.015	
		(7) elution	1.0	0.015 to 0.0	linear
		(8) elution	10	0.0	

Fractograms using the UV−vis detector at 450 and 600 nm were obtained. The diffuse reflectance as the absorbance of the soil free of CB was also measured.

Filter-Aided CB Recovery and Re-Dispersion. Once CB was isolated by using the dispersive media, 1.5 mL of each bulk dispersion (300 mg·L^{-1}) was passed through the different filter membranes using a 2.5 mL syringe and a Swinnex filter holder from Merck. The supernatant was collected and injected in the AF4 system diluted 1/2 for polymeric dispersion and 1/8 for biological dispersion. For SdF3-MALS analysis, samples were directly injected after the filtering step. Recoveries were calculated by comparing the AF4-DLS response of a CB standard with the response of CB-filtered solution. Figure S.1 of the Supporting Information shows the complete filter-aided recovery procedure.

CB isolated from soil samples was also filtered using membranes of fiberglass (2.00 μm), nylon (0.45 μm), and Teflon (0.10 μm). The filtered solution was collected and injected in the AF4 system diluted 1/2 for polymeric dispersion and 1/8 for biological dispersion. For SdF3-MALS analysis, samples were directly injected after the filtering step.

Re-dispersion of CB recovered in the filter was carried out using a shaking procedure for 4 h using 1.5 mL of the corresponding dispersant. Then, an aliquot of the dispersion was injected in the AF4-DLS system.

For diffuse reflectance analysis, 400 μL of CB or pigment paste dispersions obtained with dilution 1/8 with the biological

https://doi.org/10.1021/acsomega.3c03857
ACS Omega 2023, 8, 34795−34804

dispersant was recovered using the 0.10 μm Teflon membrane. Then, the filter sample was measured using a Cary 60 UV−vis spectrophotometer equipped with a diffuse reflection probe.

■ ASSOCIATED CONTENT

Supporting Information

The Supporting Information is available free of charge at https://pubs.acs.org/doi/10.1021/acsomega.3c03857.

Figure S.1: filter-based extraction procedure; Figure S.2: ligand exchange study and filter-aided recovery assay using fiberglass (2 μm) as a support (mountain A soil as the matrix) and ligand exchange study and filter-aided recovery assay using fiberglass (2 μm) as a support (orchard A soil as the matrix); Figure S.3: filter-based analysis of CB dispersion from sample N326 prepared with a polymeric dispersant using different filters (fiberglass, 2.00 μm; fiberglass, 1.00 μm; nylon, 5 μm; nylon, 0.45 μm; Teflon, 0.10 μm; Teflon, 0.10 μm); Figure S.4: filter-based analysis of CB dispersion from sample N326 prepared with a biological dispersant using different filters (fiberglass, 2.00 μm; fiberglass, 1.00 μm; fiberglass, 0.70 μm; nylon, 0.45 μm; nylon, 0.22 μm; Teflon, 0.45 μm; Teflon, 0.20 μm; Teflon, 0.10 μm); Table S.1: soil particle size composition obtained from optical microscopy; Table S.2: organic matter obtained by the gravimetric method (n = 3) (PDF)

■ AUTHOR INFORMATION

Corresponding Author

Pilar Campíns-Falcó − *MINTOTA Research Group, Departament de Química Analítica, Facultat de Química, Universitat de Valencia, 46100 Burjassot, Spain;* orcid.org/0000-0002-0980-8298; Email: pilar.campins@uv.es

Authors

Lorenzo Sanjuan-Navarro − *MINTOTA Research Group, Departament de Química Analítica, Facultat de Química, Universitat de Valencia, 46100 Burjassot, Spain;* orcid.org/0000-0001-5594-5130

Aaron Boughbina-Portolés − *MINTOTA Research Group, Departament de Química Analítica, Facultat de Química, Universitat de Valencia, 46100 Burjassot, Spain*

Yolanda Moliner-Martínez − *MINTOTA Research Group, Departament de Química Analítica, Facultat de Química, Universitat de Valencia, 46100 Burjassot, Spain*

Frank von der Kammer − *Department of Environmental Geosciences, University of Vienna, 1090 Vienna, Austria;* orcid.org/0000-0002-8653-6687

Complete contact information is available at: https://pubs.acs.org/10.1021/acsomega.3c03857

Author Contributions

The manuscript was written through contributions of all authors.

Notes

The authors declare no competing financial interest.

■ ACKNOWLEDGMENTS

The authors acknowledge Birla Carbon (Cantabria, Spain) as a CB supplier. This work was supported by EU FEDER, Gobierno de España MCIU-AEI (PID2021-124554NB-I00), Generalitat Valenciana (PROMETEO Program 2020/109), and EU FEDER-Generalitat Valenciana (ID-FEDER/2018/049). L.S.-N. expresses his gratitude for the FPU-grant (MCIU-AEI) and A.B.-P. to the Generalitat Valenciana for the grant (grantCIACIF/2021/069).

■ REFERENCES

(1) Singh, A.K. Introduction to Nanoparticles and Nanotoxicology. In *Engineered Nanoparticles*; 2016, Boston, pp. 1−18, DOI: 10.1016/B978-0-12-801406-6.00001-7.

(2) Xu, K.; Wang, X.; Lu, C.; Liu, Y.; Zhang, D.; Cheng, J. Toxicity of three carbon-based nanomaterials to earthworms: Effect of morphology on biomarkers, cytotoxicity, and metabolomics. *Sci. Total Environ.* **2021**, *777*, No. 146224.

(3) Chaudhuri, I.; Fruijtier-Pölloth, C.; Ngiewih, Y.; Levy, L. Evaluating the evidence on genotoxicity and reproductive toxicity of carbon black: a critical review. *Crit. Rev. Toxicol.* **2018**, *48*, 143.

(4) Piccinno, F.; Gottschalk, F.; Seeger, S.; Nowack, B. Industrial production quantities and uses of ten engineered nanomaterials in Europe and the world. *J. Nanopart. Res.* **2012**, *14*, DOI: 10.1007/s11051-012-1109-9.

(5) González-Fuenzalida, R. A.; Sanjuan-Navarro, L.; Moliner-Martínez, Y.; Campíns-Falcó, P. Quantitative study of the capture of silver nanoparticles by several kinds of soils. *Sci. Total Environ.* **2018**, *630*, 1226.

(6) Mottier, A.; Mouchet, F.; Pinelli, É.; Gauthier, L.; Flahaut, E. Environmental impact of engineered carbon nanoparticles: from releases to effects on the aquatic biota. *Curr. Opin. Biotechnol.* **2017**, *46*, 1.

(7) Sanjuan-Navarro, L.; Moliner-Martínez, Y.; Campíns-Falcó, P. The state of art of nanocarbon black as analyte of interest in several matrices: a review. *TrAC, Trends Anal. Chem.* **2022**, *157*, No. 116769.

(8) Silva, T. A.; Moraes, F. C.; Janegitz, B. C.; Fatibello-Filho, O.; Ganta, D. Electrochemical biosensors based on nanostructured carbon black: A review. *J. Nanomater.* **2017**, *2017*, 1.

(9) Bae, J.; Kim, W.; Rah, K.; Jung, E. C.; Lee, S. Application of flow field-flow fractionation (FlFFF) for size characterization of carbon black particles in ink. *Microchem. J.* **2012**, *104*, 44.

(10) Yee, M. J.; Mubarak, N. M.; Abdullah, E. C.; Khalid, M.; Walvekar, R.; Karri, R. R.; Nizamuddin, S.; Numan, A. Carbon nanomaterials based films for strain sensing application—A review. *Nano-Struct. Nano-Objects* **2019**, *18*, No. 100312.

(11) Uddin, M.N.; Rahman, M.M.; Asmatulu, R. Recent Progress on Synthesis, Characterization and Applications of Carbon Black Nanoparticles. In *Advances in Nanotechnology*; Bertul, Z., Trenor, J., Eds.; Nova Science Publishers, 2017; Vol. *19*, pp. 40−78.

(12) Samaržija-Jovanović, S.; Jovanović, V.; Marković, G.; Marinović-Cincović, M. The effect of different types of carbon blacks on the rheological and thermal properties of acrylonitrile butadiene rubber. *J. Therm. Anal. Calorim.* **2009**, *98*, 275.

(13) Wang, M.-J.; Gray, C.A.; Reznek, S.A.; Mahmud, K.; Kutsovsky, Y. CARBON BLACK. In *Kirk-Othmer Encyclopedia of Chemical Technology*; New York, 2003; pp. 761−803.

(14) Maynard, A. D.; Aitken, R. J.; Butz, T.; Colvin, V.; Donaldson, K.; Oberdörster, G.; Philbert, M. A.; Ryan, J.; Seaton, A.; Stone, V.; et al. Safe handling of nanotechnology. *Nature* **2006**, 444.

(15) Nowack, B.; Bucheli, T. D. Occurrence, behavior and effects of nanoparticles in the environment. *Environ. Pollut.* **2007**, *150*, 5.

(16) Navarro, E.; Baun, A.; Behra, R.; Hartmann, N. B.; Filser, J.; Miao, A. J.; Quigg, A.; Santschi, P. H.; Sigg, L. Environmental behavior and ecotoxicity of engineered nanoparticles to algae, plants, and fungi. *Ecotoxicology* **2008**, *17*, 372.

(17) Canesi, L.; Ciacci, C.; Betti, M.; Fabbri, R.; Canonico, B.; Fantinati, A.; Marcomini, A.; Pojana, G. Immunotoxicity of carbon black nanoparticles to blue mussel hemocytes. *Environ. Int.* **2008**, *34*, 1114.

(18) Rodd, A. L.; Creighton, M. A.; Vaslet, C. A.; Rangel-Mendez, J. R.; Hurt, R. H.; Kane, A. B. Effects of surface-engineered

nanoparticle-based dispersants for marine oil spills on the model organism Artemia franciscana. *Environ. Sci. Technol.* **2014**, *48*, 6419.
(19) Xu, K.; Liu, Y. X.; Wang, X. F.; Li, S. W.; Cheng, J. M. Combined toxicity of functionalized nano-carbon black and cadmium on Eisenia fetida coelomocytes: The role of adsorption. *J. Hazard. Mater.* **2020**, *398*, No. 122815.
(20) Xu, K.; Liu, Y. X.; Wang, X. F.; Cheng, J. M. Effect of Nano-Carbon Black Surface Modification on Toxicity to Earthworm (Eisenia fetida) Using Filter Paper Contact and Avoidance Test. *Bull. Environ. Contam. Toxicol.* **2019**, *103*, 206.
(21) Myojo, T.; Ono-Ogasawara, M. Review; risk assessment of aerosolized SWCNTs, MWCNTs, fullerenes and carbon black. *Kona Powder Part. J.* **2018**, *35*, 80.
(22) Jia, G.; Wang, H.; Yan, L.; Wang, X.; Pei, R.; Yan, T.; Zhao, Y.; Guo, X. Cytotoxicity of carbon nanomaterials: Single-wall nanotube, multi-wall nanotube, and fullerene. *Environ. Sci. Technol.* **2005**, *39*, 1378.
(23) Kim, K.; Lee, S.; Kim, W. Characterization of carbon black nanoparticles using asymmetrical flow field-flow fractionation (AsFlFFF). *Anal. Sci. Technol.* **2019**, *32*, DOI: 10.5806/AST.2019.32.3.77.
(24) Sun, S.; Liu, Z. D.; Diao, P. Preparation and catalytic studies of pyrrole-doped carbon black oxide cathode materials for oxygen reduction reactions. *Gongcheng Kexue Xuebao/Chinese J. Eng.* **2019**, *41*, DOI: 10.13374/j.issn2095-9389.2019.02.008.
(25) Sanjuan-Navarro, L.; Boughbina-Portolés, A.; Moliner-Martínez, Y.; Campíns-Falcó, P. Aqueous Dilution of Noble NPs Bulk Dispersions: Modeling Instability due to Dissolution by AF4 and Stablishing Considerations for Plasmonic Assays. *Nanomaterials* **2020**, *10*, 1802.
(26) Boughbina-Portolés, A.; Sanjuan-Navarro, L.; Moliner-Martínez, Y.; Campíns-Falcó, P. Study of the stability of citrate capped agnps in several environmental water matrices by asymmetrical flow field flow fractionation. *Nanomaterials* **2021**, *11*, DOI: 10.3390/nano11040926.
(27) Sanjuan-Navarro, L.; Moliner-Martínez, Y.; Campíns-Falcó, P. Characterization and Quantification of Carbon Black Nanomaterials in Polymeric and Biological Aqueous Dispersants by Asymmetrical Flow Field Flow fractionation. ACS. *Omega* **2021**, *6*, 31822.
(28) Han, Y.; Hwang, G.; Park, S.; Gomez-Flores, A.; Jo, E.; Eom, I. C.; Tong, M.; Kim, H. J.; Kim, H. Stability of carboxyl-functionalized carbon black nanoparticles: the role of solution chemistry and humic acid. *Environ. Sci.: Nano* **2017**, *4*, 800.
(29) Lohwacharin, J.; Takizawa, S.; Punyapalakul, P. Carbon black retention in saturated natural soils: Effects of flow conditions, soil surface roughness and soil organic matter. *Environ. Poll.* **2015**, *205*, 131.
(30) Bismarck, A.; Boccaccini, A. R.; Egia-Ajuriagojeaskoa, E.; Hülsenberg, D.; Leutbecher, T. Surface characterization of glass fibers made from silicate waste: Zeta-potential and contact angle measurements. *J. Mater. Sci.* **2004**, *39*, 401.
(31) Xu, Z.; Mahalingam, S.; Rohn, J. L.; Ren, G.; Edirisinghe, M. Physio-chemical and antibacterial characteristics of pressure spun nylon nanofibres embedded with functional silver nanoparticles. *Mater. Sci. Eng. C* **2015**, *56*, 195.
(32) Dong, D. Fiberglass Surface and Its Electrokinetic Properties. *Int. Nonwovens J.* **1999**, os-8.
(33) *Joint Committee for Guides in Metrology (JCGM) 100:2008. Evaluation of measurement data — Guide to the expression of uncertainty in measurement.* https://www.bipm.org/documents/20126/2071204/JCGM_100_2008_E.pdf/cb0ef43f-baa5-11cf-3f85-4dcd86f77bd6.

https://doi.org/10.1021/acsomega.3c03857
ACS Omega 2023, 8, 34795−34804